

# Hawking time crystal

Juan Ramón Muñoz de Nova and Fernando Sols

*Departamento de Física de Materiales, Universidad Complutense de Madrid, E-28040 Madrid, Spain*

(Dated: July 16, 2025)

We report the numerical observation of a time crystal in a quantum black-hole laser (BHL), where the genuine spontaneous character of the symmetry breaking stems from the self-amplification of spontaneous Hawking radiation. The resulting Hawking time crystal (HTC) is characterized by the periodic dependence of the out-of-time density-density correlation function, while equal-time correlations are time-independent because they embody averages over different realizations with a random oscillation phase. The HTC can be regarded as a nonlinear periodic version of the Andreev-Hawking effect, signaled by anticorrelation bands resulting from the spontaneous, quantum emission of pairs of dispersive waves and solitons into the upstream and downstream regions.

*Introduction.*— The field of analogue gravity [1] investigates the simulation of otherwise inaccessible gravitational phenomena by using a variety of tabletop experiments, including atomic condensates [2, 3], nonlinear optical fibers [4, 5], ion rings [6, 7], water waves [8, 9], quantum fluids of light [10, 11], superconducting transmon qubits [12], or superfluid helium [13]. This has resulted in observations of the dynamical Casimir effect [14], Sakharov oscillations [15], superradiance [16], inflation [17], Unruh effect [18], quasinormal ringdown [19], backreaction [20], or cosmological particle creation [21, 22]. A central topic is the observation of spontaneous Hawking radiation [23–38], finally achieved in atomic condensates [39–41], manifested as the correlated quantum emission of Bogoliubov quasiparticles from a subsonic/supersonic interface playing the role of the event horizon. Since scattering within the supersonic region also provides a bosonic analogue of the Andreev effect [42], by borrowing concepts from quantum optics [43] the whole process can be understood as a joint Andreev-Hawking effect [44].

A major remaining challenge is the achievement of a black-hole laser (BHL) [45–60], where Hawking radiation is self-amplified by successive reflections between a pair of horizons. Of particular interest is the late-time behavior of a BHL, after the initial instability has saturated, where it may exhibit a periodic regime of continuous emission of solitons (CES) [52, 56], representing the *bona-fide* BHL [52]. Indeed, the CES state is a universal feature of flowing condensates, providing one of the simplest realizations of the more general concept of spontaneous Floquet state: a state of a time-independent Hamiltonian which oscillates like a Floquet state due to interactions [61]. Among other intriguing features, spontaneous Floquet states display temporal Floquet-Nambu-Goldstone (FNG) modes with zero-quasifrequency, whose quantum amplitude represents a unique tangible realization of time operator in Quantum Mechanics [62]. This connects with the field of time crystals [63, 64], where both discrete [65–67] and continuous time crystals [68–72] have already been observed in a variety of systems [73–87].

So far, spontaneous Floquet states have emerged only within mean-field descriptions, imposing a global time origin. Hence, even though there is a temporal FNG mode, technically speaking the symmetry breaking of time-translation invariance is not truly spontaneous. Here we show that a *bona-fide* quantum, continuous time crystal can be achieved by leveraging the quantum nature of the spontaneous Hawking radiation self-amplified in a BHL. Furthermore, we argue that an HTC represents a nonlinear periodic version of the Andreev-Hawking effect.

*BHL model.*— We take the flat-profile BHL (FPBHL) model as a test ground since, due to its simplicity, neatly captures the physics at play [25, 52, 60, 88]. For  $t < 0$ , a 1D homogeneous atomic quasicondensate [89] flows from left to right, described by a stationary Gross-Pitaevskii (GP) wavefunction  $\Psi_0(x) = \sqrt{n_0}e^{iqx}$ . The corresponding flow and sound speeds are  $v = \hbar q/m < c_0 = \sqrt{gn_0/m}$ , where  $g$  is the coupling constant describing the short-ranged interactions between atoms and  $m$  is their mass. Hereafter,  $\hbar = m = c_0 = 1$ , and the GP wavefunction is rescaled as  $\Psi(x, t) \rightarrow \sqrt{n_0}\Psi(x, t)$ . For  $t \geq 0$ , the external potential and the coupling constant are inhomogeneously quenched so that the condensate becomes supersonic for  $|x| < L/2$ , with sound speed  $c_2 < v$ , while  $\Psi_0(x)$  remains stationary. Hence, a BHL configuration is reached, presenting two sonic horizons at  $x = \pm L/2$ , Fig. 1a.

A BHL is characterized by the emergence of a finite Bogoliubov spectrum of complex frequencies. We focus on short cavities containing only one degenerate unstable mode with purely imaginary frequency  $i\Gamma$ , whose quantum amplitude  $\hat{X}$  behaves as the position operator associated to the annihilation operator of a degenerate parametric amplifier [44]. This optimal cavity choice both maximizes the growth rate  $\Gamma$  and minimizes the transient towards the final state [52, 60, 88]. Once excited, the lasing amplitude is exponentially amplified up to the saturation regime, where interactions become critical. In general, a condensate flowing over some obstacle with velocity  $v$  above certain critical velocity  $v_c$  asymptotically approaches the CES state [61],

$$\Psi(x, t) \xrightarrow[t \rightarrow \infty]{} e^{-i\mu t} \Psi_0(x, t), \quad (1)$$

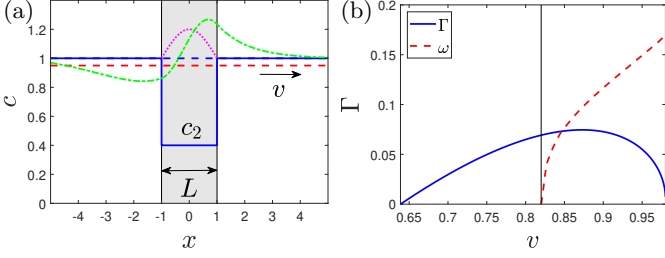


FIG. 1. (a) Spatial profile of sound (solid blue) and flow (dashed red) velocities of the FPBHL at  $t = 0$ . Horizontal dashed blue line represents the homogeneous initial condition  $\Psi_0(x) = e^{ivx}$ . The shaded area indicates the lasing cavity where the coupling constant is quenched for  $t \geq 0$  so that  $c(x) = c_2$  (solid blue line). A small bump of amplitude  $A$  (dotted magenta) is added within the lasing cavity to the initial condition in order to coherently stimulate the unstable mode (dashed-dotted green). (b) Velocity dependence of  $\Gamma$  (solid blue) and  $\omega$  (dashed red) for fixed  $c_2 = 0.4, L = 2$ . Vertical line marks the critical velocity  $v = v_c$ .

where  $\mu$  is the quasichemical potential and  $\Psi_0(x, t)$  is a periodic function,  $\Psi_0(x, t) = \Psi_0(x, \phi_0 + \omega t)$ , with  $\Psi_0(x, \phi + 2\pi) = \Psi_0(x, \phi)$  and  $\omega = 2\pi/T$ . The dependence of  $\Gamma, \omega$  with respect to  $v$  for a FPBHL is shown in Fig. 1b. Due to the time-independence of the underlying Hamiltonian, the CES state is a spontaneous Floquet state, where the oscillation phase-shift  $\phi_0$  is not *a priori* fixed, in contrast to conventional Floquet systems, leading to the emergence of a temporal FNG mode in the Bogoliubov spectrum [62].

*Hawking time crystal.*— In order to achieve a genuine spontaneous temporal symmetry breaking, we explore the classical-quantum crossover of the BHL [60] by adding a small perturbation within the lasing cavity (dotted magenta in Fig. 1a). Specifically, the GP wavefunction at  $t = 0$  now reads  $\Psi(x, 0) = [1 + A\delta\Psi_C(x)] e^{ivx}$ , with  $\delta\Psi_C(x) = \cos(\pi x/L)\theta(x + L/2)\theta(L/2 - x)$  and  $\theta$  the Heaviside function. This perturbation provides a coherent, classical amplitude to the density modulation associated to the lasing mode (dashed-dotted green), mimicking the presence of Bogoliubov-Cherenkov-Landau radiation [90] in real experiments [41, 91, 92]. Regarding the quantum state, we take the zero-temperature ground state in the comoving frame [93]. For large  $A$ , the dynamics is described by a Bogoliubov approximation of small quantum fluctuations around the mean-field trajectory generated by the amplification of the coherent lasing amplitude; for small  $A$ , the dynamics is governed by the squeezing of the initial vacuum. Hence,  $A$  is a control parameter of the classical-quantum crossover.

The time evolution of both the condensate and its quantum fluctuations is computed via the Truncated Wigner (TW) method [94], a quantum Monte Carlo technique used in both analogue gravity [25, 40, 60, 95, 96] and time crystals [82]; here we consider ensembles of

$N_{\text{stat}} = 1000$  simulations. We evaluate the ensemble-averaged density

$$n(x, t) \equiv \langle \hat{n}(x, t) \rangle = \langle \hat{\Psi}^\dagger(x, t) \hat{\Psi}(x, t) \rangle, \quad (2)$$

and the second-order correlation function

$$\begin{aligned} g^{(2)}(x, x', t, t') &\equiv \langle \hat{\Psi}^\dagger(x, t) \hat{\Psi}^\dagger(x', t') \hat{\Psi}(x', t') \hat{\Psi}(x, t) \rangle \\ &- n(x, t)n(x', t'). \end{aligned} \quad (3)$$

We distinguish between the *equal-time* correlation function (ETCF)  $g^{(2)}(x, x', t) \equiv g^{(2)}(x, x', t, t)$  and the *out-of-time* correlation function (OTCF)  $g^{(2)}(x, x', \tau; t) \equiv g^{(2)}(x, x', t, t + \tau)$ .

Figs. 2a-c, e-g show  $n(x, t)$  and  $g^{(2)}(x, x', t)$  for decreasing  $A = 0.05, 0.005, 0$ , respectively. For large  $A$ , Figs. 2a,e, a good agreement is found with the Bogoliubov prediction

$$\begin{aligned} n(x, t) &\simeq n_0(x, t) \equiv |\Psi_0(x, t)|^2, \\ g^{(2)}(x, x', t) &\simeq \partial_t n_0(x, t) \partial_t n_0(x', t) C(t), \end{aligned} \quad (4)$$

with  $C(t)$  a quadratic function accounting for the linear growth of the quantum amplitude of the temporal FNG mode [62]. The neat, sharp features of the background CES state are thus imprinted on the density and the ETCF; those are smeared out when approaching the quantum regime. Specifically, in a purely quantum BHL (i.e.,  $A = 0$ ), Figs. 2c,g, there is no well-defined mean-field trajectory and  $\phi_0$  is spontaneously chosen in each TW realization. If we assume a uniform phase-shift distribution, ensemble averages then represent averages over the time origin  $t_0 = \phi_0/\omega \in [0, T)$  within a period, resulting in time-independent values  $n(x, t) = n_{\text{HTC}}(x)$  and  $g^{(2)}(x, x', t) = g_{\text{HTC}}^{(2)}(x, x', \tau = 0)$ , with

$$\begin{aligned} n_{\text{HTC}}(x) &= \frac{1}{T} \int_0^T dt_0 n_0(x, t_0), \\ g_{\text{HTC}}^{(2)}(x, x', \tau) &= \frac{1}{T} \int_0^T dt_0 n_0(x, t_0 + \tau) n_0(x', t_0) \\ &- n_{\text{HTC}}(x) n_{\text{HTC}}(x'). \end{aligned} \quad (5)$$

An excellent agreement with this theoretical prediction is found at late times for both density (Figs. 2c,d) and ETCF (Figs. 2g,h).

The system periodicity is manifested through the OTCF,  $g^{(2)}(x, x', \tau; t) = g_{\text{HTC}}^{(2)}(x, x', \tau) = g_{\text{HTC}}^{(2)}(x, x', \tau + T)$ , displayed in Figs. 2i,j for  $\tau = 10, 20$  and fixed  $t = 870$ . As a figure of merit for the OTCF periodicity, we choose the Fourier transform in the upstream-downstream quadrant ( $x > 0, x' < 0$ ) evaluated at the peak of the spectrum,  $\mathcal{G}(t, t')$ , and normalized so that  $\mathcal{G}_{\text{HTC}}(\tau = 0) = 1$ . The real part of  $\mathcal{G}(t, t')$  is shown in Fig. 2k; the imaginary part displays a similar behavior. We observe that, at late times,  $\mathcal{G}(t, t')$  becomes a sole function of  $t - t'$  (diagonal fringes). The inset shows the

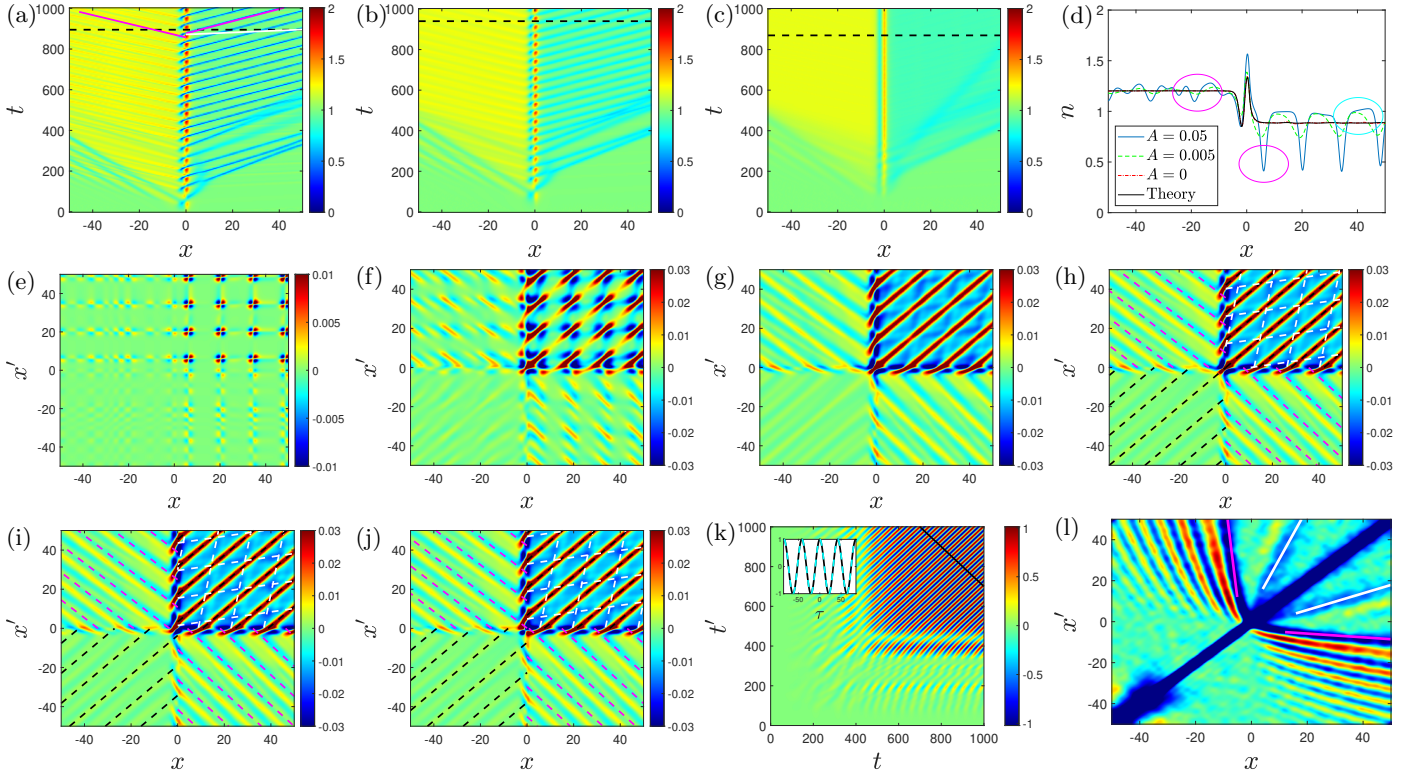


FIG. 2. Expectation values for a FPBHL with  $v = 0.95, c_2 = 0.4, L = 2$ , computed with the TW method. (a)-(c) Ensemble-averaged density  $n(x, t)$  for initial classical amplitudes  $A = 0.05, 0.005, 0$ , respectively. (d) Snapshots of  $n(x, t)$  at the times indicated by horizontal dashed line in (a)-(c). Black line is the theoretical prediction  $n_{\text{HTC}}(x)$ , Eq. (5). (e)-(g) ETCF  $g^{(2)}(x, x', t)$  for (a)-(c), evaluated at the times shown in (d). (h) Theoretical ETCF  $g^{(2)}_{\text{HTC}}(x, x', \tau = 0)$ , Eq. (5). (i)-(j) OTCF  $g^{(2)}(x, x', \tau; t)$  for  $A = 0$ , evaluated at  $\tau = 10, 20$  and fixed  $t = 870$ . (k)  $\text{Re } G(t, t')$ . Inset: 1D profile along the black line in the main plot. Dashed cyan is the theoretical prediction  $\text{Re } G_{\text{HTC}}(\tau)$ . l) Spatial structure of the ETCF for a flat-profile black hole with  $v = 0.95, c_2 = 0.4$  [27]. Magenta (white) solid lines indicate the Hawking (Andreev) correlation bands.

1D profile along the black line of the main plot, in great agreement with the theoretical prediction (dashed cyan).

The suppression of the time-dependence of the density and the ETCF, as well as the periodic nature of the OTCF, are the characteristic hallmarks of a *bona-fide* time crystal [97], here revealing the formation of an HTC, i.e., a continuous time crystal whose spontaneous symmetry breaking results from the self-amplification of spontaneous Hawking radiation.

*Nonlinear Andreev-Hawking.*— The spatial structure of the correlations in Fig. 2 reflects that of the CES state, characterized by the periodic emission of dispersive waves/solitons into the upstream/downstream regions, whose trajectory is well fitted by a ballistic motion  $x_{u,d}(t) = x_{u,d}^{(0)} \mp v_{u,d}t$ , with  $v_{u,d} > 0$  (magenta lines, circles in Fig. 2a,d, respectively). Simultaneously, another traveling wave is emitted into the downstream region, with trajectory  $x_w(t) = x_w^{(0)} + v_w t$  (white line, cyan circle in Fig. 2a,d).

From Eq. (5), strong self-correlations between the upstream waves/downstream solitons and their past and future counterparts are predicted for the OTCF along

the diagonals

$$\frac{x - x'}{v_{u,d}} = \tau + nT, \quad n \in \mathbb{Z}, \quad (6)$$

dashed black lines in Figs. 2h,i,j. In turn, the density defect carried by a soliton is correlated with the positive amplitude of the emitted upstream and downstream waves, spawning the anticorrelation bands

$$\begin{aligned} \frac{x'}{v_u} + \frac{x}{v_d} &= \frac{x_u^{(0)}}{v_u} + \frac{x_d^{(0)}}{v_d} + \tau + nT, \\ \frac{x'}{v_w} - \frac{x}{v_d} &= \frac{x_w^{(0)}}{v_w} - \frac{x_d^{(0)}}{v_d} + \tau + nT, \quad n \in \mathbb{Z}. \end{aligned} \quad (7)$$

The expression for the remaining correlation features is obtained by exchanging  $x \leftrightarrow x'$  and  $\tau \rightarrow -\tau$ . Upper (lower) Eq. (7) is indicated by dashed magenta (white) lines in Figs. 2h,i,j, in good agreement with the numerically observed patterns. The dispersive nature of the upstream wave gives rise to the yellow bands parallel to the dashed magenta lines, representing the positive correlation between the wave and soliton minima (magenta circles in Fig. 2d).

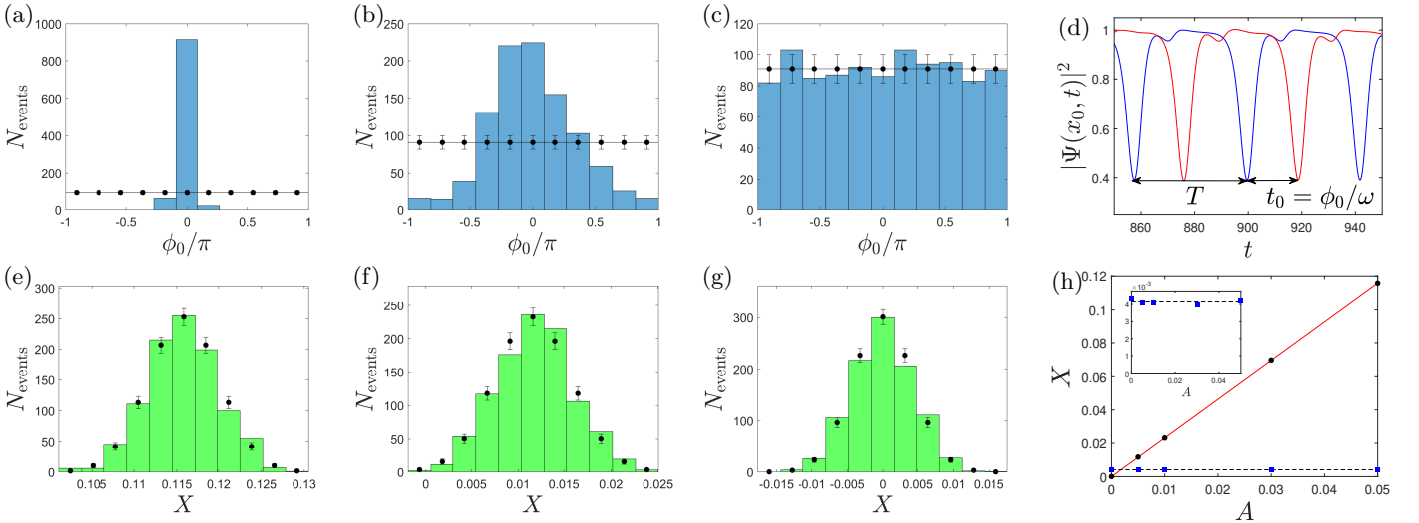


FIG. 3. (a)-(c) Histogram of the oscillation phase  $\phi_0$  for the TW ensembles of Figs. 2a-c, respectively. Horizontal line with error bars indicates a uniform distribution and its statistical uncertainty. (d) Schematic obtention of  $\phi_0$ , where blue line is the mean-field trajectory and red line is a particular TW realization. (e)-(g) Histogram of the lasing amplitude  $X$  at  $t = 0$  for (a)-(c). Dots with error bars indicate the expected Gaussian distribution (8) and its statistical uncertainty. (h)  $X_C$  (black dots) and  $X_Q$  (blue squares) as a function of  $A$ . Solid red, horizontal dashed black lines are the theoretical predictions for  $X_C, X_Q$ . Inset: Zoom of  $X_Q$ .

Remarkably, these anticorrelation bands are a nonlinear version of those arising from the spontaneous Andreev-Hawking effect [27], Fig. 2l. The celebrated Hawking moustache (magenta line) results from the correlated emission of the partner and Hawking modes into the downstream/upstream region, respectively. Parallel fringes to the main moustache again emerge due to dispersive effects. The Andreev band (white line) results from the correlation of the anomalous partner mode with the remaining normal, copropagating mode in the downstream region. In an HTC, the analogue of a partner mode is a soliton, correlative emitted along with one wave upstream (Hawking) and one downstream (Andreev). Their correlation patterns become spatially periodic as a result of the time-periodicity of the HTC and their ballistic traveling nature.

*Classical-quantum crossover.*— More information on the spontaneous symmetry breaking is revealed by the statistics of the oscillation phase  $\phi_0$  within the TW ensemble, Figs. 3a-c, obtained by examining the soliton passage in the late-time density  $|\Psi(x_0, t)|^2$  at a fixed point  $x = x_0 > 0$ , Fig. 3d. As a reference, we set  $\phi_0 = 0$  for the mean-field wavefunction; for a purely quantum BHL, we choose  $A = 0.003$  as mean-field reference. The frequency is quite stable within the TW ensemble, and the results do not depend significantly on the value of  $x_0$  or the bin number (not shown). As expected, the phase distribution broadens in the purely quantum limit, Fig. 3c, approaching a uniform distribution (horizontal line).

The late distribution of  $\phi_0$  in the CES state is determined by the initial distribution of the lasing amplitude

$X$ , whose Wigner function is Gaussian,

$$W(X) = \frac{1}{\sqrt{2\pi X_Q^2}} e^{-\frac{(X-X_C)^2}{2X_Q^2}}. \quad (8)$$

The mean  $X_C \propto A$  is the classical, coherent component of the lasing amplitude, while the standard deviation  $X_Q \propto n_0^{-1/2}$  controls its quantum fluctuations, as expected from general scaling arguments [60]. The TW histogram for  $X$  at  $t = 0$  is shown in Figs. 3e-g, in excellent agreement with the expected Gaussian distribution (black dots with error bars). The  $X_C, X_Q$  values obtained from the histograms are depicted in Fig. 3h as a function of  $A$ .

In each realization, the saturation regime is reached at times  $t$  when  $X e^{\Gamma t} \sim 1$ . Fluctuations in  $X$  are thus translated into fluctuations in  $t$ , and consequently in  $\phi_0$ . In the classical limit,  $X = X_C + \delta X$  with  $\delta X \sim X_Q \ll X_C$ , so

$$\phi_0 \simeq -\frac{\omega}{\Gamma} \frac{\delta X}{X_C} \sim \frac{\omega}{\Gamma} \frac{X_Q}{X_C}, \quad (9)$$

while in the quantum limit  $X_C \ll X_Q$ ,

$$\phi_0 \sim -\frac{\omega}{\Gamma} \ln |X|. \quad (10)$$

The width  $\Delta\phi_0$  of the time-shift fluctuations is then controlled by  $X_Q$  and  $\omega/\Gamma$ , which must satisfy  $\omega/\Gamma \gg 1$  to achieve a fully spontaneous HTC. Even though we have focused on the HTC emerging from the seemingly fine-tuned case of  $A \ll 1$  and zero temperature, thermal

and experimental fluctuations in real setups will actually broaden the lasing distribution as  $X_Q^2 \rightarrow X_Q^2 + X_T^2 + X_E^2$ , with  $X_T^2, X_E^2$  the contribution from thermal and experimental fluctuations, further reinforcing the spontaneous character of the temporal symmetry breaking. Moreover, the robustness of the HTC is ensured by that of the CES state [61], certifying the time-crystalline nature of the HTC.

*Conclusions.*—We have numerically observed an HTC, i.e., a time crystal whose spontaneous symmetry breaking results from the self-amplification of spontaneous Hawking radiation. The HTC is characterized by time-independent expectation values for both the density and the ETCF, and by a time-periodic OTCF. Interestingly, an HTC can be regarded as a nonlinear version of the Andreev-Hawking effect.

The formation of an HTC further demonstrates how analogue concepts can inspire applications in tabletop experiments, in addition to quantum amplifiers [60] or low-pass filters [98, 99]. Conversely, an HTC and the associated nonlinear Andreev-Hawking effect represent novel concepts in the analogue field, increasing the intrinsic interest of a potential BHL observation. Moreover, this work highlights the conceptual richness of spontaneous Floquet states. Our results can be translated into other systems governed by similar nonlinear equations of motion, such as nonlinear optical fibers or polariton superfluids [5, 10, 11, 100, 101]. From a broader perspective, the realization of a time operator [62] within a gravitational analogue scenario is of fundamental interest, since it provides a novel and tangible platform for foundational research on the quantum nature of time, including potential connections to quantum gravity.

This work has received funding from European Union’s Horizon 2020 research and innovation programme under the Marie Skłodowska-Curie Grant Agreement No. 847635, and from Spain’s Agencia Estatal de Investigación through Grant No. PID2022-139288NB-I00.

- 
- [1] W. G. Unruh, *Phys. Rev. Lett.* **46**, 1351 (1981).
  - [2] L. J. Garay, J. R. Anglin, J. I. Cirac, and P. Zoller, *Phys. Rev. Lett.* **85**, 4643 (2000).
  - [3] O. Lahav, A. Itah, A. Blumkin, C. Gordon, S. Rinott, A. Zayats, and J. Steinhauer, *Phys. Rev. Lett.* **105**, 240401 (2010).
  - [4] F. Belgiorno, S. L. Cacciatori, M. Clerici, V. Gorini, G. Ortenzi, L. Rizzi, E. Rubino, V. G. Sala, and D. Faccio, *Phys. Rev. Lett.* **105**, 203901 (2010).
  - [5] J. Drori, Y. Rosenberg, D. Bermudez, Y. Silberberg, and U. Leonhardt, *Phys. Rev. Lett.* **122**, 010404 (2019).
  - [6] B. Horstmann, B. Reznik, S. Fagnocchi, and J. I. Cirac, *Phys. Rev. Lett.* **104**, 250403 (2010).
  - [7] M. Wittemer, F. Hakelberg, P. Kiefer, J.-P. Schröder, C. Fey, R. Schützhold, U. Warring, and T. Schaetz, *Phys. Rev. Lett.* **123**, 180502 (2019).
  - [8] S. Weinfurtner, E. W. Tedford, M. C. J. Penrice, W. G. Unruh, and G. A. Lawrence, *Phys. Rev. Lett.* **106**, 021302 (2011).
  - [9] L.-P. Euvé, F. Michel, R. Parentani, T. G. Philbin, and G. Rousseaux, *Phys. Rev. Lett.* **117**, 121301 (2016).
  - [10] I. Carusotto and C. Ciuti, *Rev. Mod. Phys.* **85**, 299 (2013).
  - [11] K. Falque, A. Delhom, Q. Glorieux, E. Giacobino, A. Bramati, and M. J. Jacquet, *Phys. Rev. Lett.* **135**, 023401 (2025).
  - [12] Y.-H. Shi, R.-Q. Yang, Z. Xiang, Z.-Y. Ge, H. Li, Y.-Y. Wang, K. Huang, Y. Tian, X. Song, D. Zheng, *et al.*, *Nature Communications* **14**, 3263 (2023).
  - [13] P. Švančara, P. Smaniotti, L. Solidoro, J. F. MacDonald, S. Patrick, R. Gregory, C. F. Barenghi, and S. Weinfurtner, *Nature* **628**, 66 (2024).
  - [14] J.-C. Jaskula, G. B. Partridge, M. Bonneau, R. Lopes, J. Ruaudel, D. Boiron, and C. I. Westbrook, *Phys. Rev. Lett.* **109**, 220401 (2012).
  - [15] C.-L. Hung, V. Gurarie, and C. Chin, *Science* **341**, 1213 (2013).
  - [16] T. Torres, S. Patrick, A. Coutant, M. Richartz, E. W. Tedford, and S. Weinfurtner, *Nature Physics* **13**, 833 (2017).
  - [17] S. Eckel, A. Kumar, T. Jacobson, I. B. Spielman, and G. K. Campbell, *Phys. Rev. X* **8**, 021021 (2018).
  - [18] J. Hu, L. Feng, Z. Zhang, and C. Chin, *Nature Physics* **15**, 785 (2019).
  - [19] T. Torres, S. Patrick, M. Richartz, and S. Weinfurtner, *Phys. Rev. Lett.* **125**, 011301 (2020).
  - [20] S. Patrick, H. Goodhew, C. Gooding, and S. Weinfurtner, *Phys. Rev. Lett.* **126**, 041105 (2021).
  - [21] J. Steinhauer, M. Abuzarli, T. Aladjidi, T. Bienaimé, C. Piekarski, W. Liu, E. Giacobino, A. Bramati, and Q. Glorieux, *Nat. Commun.* **13**, 2890 (2022).
  - [22] C. Viermann, M. Sparn, N. Liebster, M. Hans, E. Kath, Á. Parra-López, M. Tolosa-Simeón, N. Sánchez-Kuntz, T. Haas, H. Strobel, *et al.*, *Nature* **611**, 260 (2022).
  - [23] U. Leonhardt, T. Kiss, and P. Öhberg, *J. Opt. B: Quantum Semiclass. Opt.* **5**, S42 (2003).
  - [24] R. Balbinot, A. Fabbri, S. Fagnocchi, A. Recati, and I. Carusotto, *Phys. Rev. A* **78**, 21603 (2008).
  - [25] I. Carusotto, S. Fagnocchi, A. Recati, R. Balbinot, and A. Fabbri, *New J. Phys.* **10**, 103001 (2008).
  - [26] J. Macher and R. Parentani, *Phys. Rev. A* **80**, 43601 (2009).
  - [27] A. Recati, N. Pavloff, and I. Carusotto, *Phys. Rev. A* **80**, 43603 (2009).
  - [28] I. Zapata, M. Albert, R. Parentani, and F. Sols, *New J. Phys.* **13**, 63048 (2011).
  - [29] P. E. Larré, A. Recati, I. Carusotto, and N. Pavloff, *Phys. Rev. A* **85**, 13621 (2012).
  - [30] J. R. M. de Nova, F. Sols, and I. Zapata, *Phys. Rev. A* **89**, 043808 (2014).
  - [31] S. Finazzi and I. Carusotto, *Phys. Rev. A* **90**, 033607 (2014).
  - [32] X. Busch and R. Parentani, *Phys. Rev. D* **89**, 105024 (2014).
  - [33] J. R. M. de Nova, F. Sols, and I. Zapata, *New J. Phys.* **17**, 105003 (2015).
  - [34] F. Michel, R. Parentani, and R. Zegers, *Phys. Rev. D* **93**, 065039 (2016).
  - [35] M. Isoard, N. Milazzo, N. Pavloff, and O. Giraud, *Phys.*

- Rev. A** **104**, 063302 (2021).
- [36] C. C. H. Ribeiro, S.-S. Baak, and U. R. Fischer, **Phys. Rev. D** **105**, 124066 (2022).
- [37] C. C. Holanda Ribeiro and U. R. Fischer, **Phys. Rev. D** **107**, L121502 (2023).
- [38] G. Ciliberto, S. Emig, N. Pavloff, and M. Isoard, **Phys. Rev. A** **109**, 063325 (2024).
- [39] J. Steinhauer, **Nature Physics** **12**, 959 (2016).
- [40] J. R. M. de Nova, K. Golubkov, V. I. Kolobov, and J. Steinhauer, **Nature** **569**, 688 (2019).
- [41] V. I. Kolobov, K. Golubkov, J. R. M. de Nova, and J. Steinhauer, **Nature Physics** **17**, 362 (2021).
- [42] I. Zapata and F. Sols, **Phys. Rev. Lett.** **102**, 180405 (2009).
- [43] D. Walls and G. Milburn, *Quantum Optics*, Springer-Link: Springer e-Books (Springer, 2008).
- [44] J. R. M. de Nova, P. F. Palacios, P. A. Guerrero, I. Zapata, and F. Sols, **Comptes Rendus. Physique** **25**, 1 (2024).
- [45] S. Corley and T. Jacobson, **Phys. Rev. D** **59**, 124011 (1999).
- [46] U. Leonhardt, T. Kiss, and P. Öhberg, **Phys. Rev. A** **67**, 33602 (2003).
- [47] C. Barceló, A. Cano, L. J. Garay, and G. Jannes, **Phys. Rev. D** **74**, 024008 (2006).
- [48] P. Jain, A. S. Bradley, and C. Gardiner, **Phys. Rev. A** **76**, 23617 (2007).
- [49] A. Coutant and R. Parentani, **Phys. Rev. D** **81**, 84042 (2010).
- [50] S. Finazzi and R. Parentani, **New J. Phys.** **12**, 095015 (2010).
- [51] D. Faccio, T. Arane, M. Lamperti, and U. Leonhardt, **Classical and Quantum Gravity** **29**, 224009 (2012).
- [52] J. R. M. de Nova, S. Finazzi, and I. Carusotto, **Phys. Rev. A** **94**, 043616 (2016).
- [53] C. Peloquin, L.-P. Euvé, T. Philbin, and G. Rousseaux, **Phys. Rev. D** **93**, 084032 (2016).
- [54] D. Bermúdez and U. Leonhardt, **Classical and Quantum Gravity** **36**, 024001 (2018).
- [55] R. Bürkle, A. Gaidoukov, and J. R. Anglin, **New Journal of Physics** **20**, 083020 (2018).
- [56] J. R. M. de Nova, P. F. Palacios, I. Carusotto, and F. Sols, **New Journal of Physics** **23**, 023040 (2021).
- [57] J. D. Rincón-Estrada and D. Bermúdez, **Annalen der Physik** **533**, 2000239 (2021).
- [58] H. Katayama, **Scientific Reports** **11**, 19137 (2021).
- [59] J. Steinhauer, **Phys. Rev. D** **106**, 102007 (2022).
- [60] J. R. M. de Nova and F. Sols, **Phys. Rev. Res.** **5**, 043282 (2023).
- [61] J. R. M. de Nova and F. Sols, **Phys. Rev. A** **105**, 043302 (2022).
- [62] J. R. M. de Nova and F. Sols, **arXiv preprint arXiv:2402.10784** (2024).
- [63] F. Wilczek, **Phys. Rev. Lett.** **109**, 160401 (2012).
- [64] K. Sacha and J. Zakrzewski, **Reports on Progress in Physics** **81**, 016401 (2017).
- [65] K. Sacha, **Phys. Rev. A** **91**, 033617 (2015).
- [66] D. V. Else, B. Bauer, and C. Nayak, **Phys. Rev. Lett.** **117**, 090402 (2016).
- [67] D. Bhowmick, H. Sun, B. Yang, and P. Sengupta, **Phys. Rev. B** **108**, 014434 (2023).
- [68] A. Syrwid, J. Zakrzewski, and K. Sacha, **Phys. Rev. Lett.** **119**, 250602 (2017).
- [69] F. Iemini, A. Russomanno, J. Keeling, M. Schirò, M. Dalmonte, and R. Fazio, **Phys. Rev. Lett.** **121**, 035301 (2018).
- [70] B. Buča, J. Tindall, and D. Jaksch, **Nature Communications** **10**, 1 (2019).
- [71] C. Booker, B. Buča, and D. Jaksch, **New Journal of Physics** **22**, 085007 (2020).
- [72] R. Daviet, C. P. Zelle, A. Rosch, and S. Diehl, **Phys. Rev. Lett.** **132**, 167102 (2024).
- [73] S. Choi, J. Choi, R. Landig, G. Kucska, H. Zhou, J. Isoya, F. Jelezko, S. Onoda, H. Sumiya, V. Khemani, et al., **Nature** **543**, 221 (2017).
- [74] J. Zhang, P. Hess, A. Kyprianidis, P. Becker, A. Lee, J. Smith, G. Pagano, I.-D. Potirniche, A. C. Potter, A. Vishwanath, et al., **Nature** **543**, 217 (2017).
- [75] S. Autti, V. B. Eltsov, and G. E. Volovik, **Phys. Rev. Lett.** **120**, 215301 (2018).
- [76] J. Smits, L. Liao, H. T. C. Stoof, and P. van der Straten, **Phys. Rev. Lett.** **121**, 185301 (2018).
- [77] J. Rovny, R. L. Blum, and S. E. Barrett, **Phys. Rev. Lett.** **120**, 180603 (2018).
- [78] A. Kyprianidis, F. Machado, W. Morong, P. Becker, K. S. Collins, D. V. Else, L. Feng, P. W. Hess, C. Nayak, G. Pagano, N. Y. Yao, and C. Monroe, **Science** **372**, 1192 (2021).
- [79] J. Randall, C. E. Bradley, F. V. van der Gronden, A. Galicia, M. H. Abobeih, M. Markham, D. J. Twitchen, F. Machado, N. Y. Yao, and T. H. Taminiau, **Science** **374**, 1474 (2021).
- [80] X. Mi, M. Ippoliti, C. Quintana, A. Greene, Z. Chen, J. Gross, F. Arute, K. Arya, J. Atalaya, R. Babbush, et al., **Nature** **601**, 531 (2022).
- [81] P. Frey and S. Rachel, **Science Advances** **8**, eabm7652 (2022).
- [82] P. Kongkhambut, J. Skulte, L. Mathey, J. G. Cosme, A. Hemmerich, and H. Kefler, **Science** **377**, 670 (2022).
- [83] D. Dreon, A. Baumgärtner, X. Li, S. Hertlein, T. Esslinger, and T. Donner, **Nature** **608**, 494 (2022).
- [84] T. Liu, J.-Y. Ou, K. F. MacDonald, and N. I. Zheludev, **Nature Physics** , 1 (2023).
- [85] A. Greilich, N. Kopteva, A. Kamenskii, P. Sokolov, V. Korenev, and M. Bayer, **Nature Physics** , 1 (2024).
- [86] I. Carraro-Haddad, D. L. Chafatinos, A. Kuznetsov, I. A. Papuccio-Fernández, A. A. Reynoso, A. Bruchhausen, K. Biermann, P. Santos, G. Usaj, and A. Fainstein, **Science** **384**, 995 (2024).
- [87] W. Wang, M. Feng, Q. Ma, Z. Cai, E. Li, and G. Liu, **Communications Physics** **8**, 191 (2025).
- [88] F. Michel and R. Parentani, **Phys. Rev. D** **88**, 125012 (2013).
- [89] C. Menotti and S. Stringari, **Phys. Rev. A** **66**, 043610 (2002).
- [90] I. Carusotto, S. X. Hu, L. A. Collins, and A. Smerzi, **Phys. Rev. Lett.** **97**, 260403 (2006).
- [91] Y.-H. Wang, T. Jacobson, M. Edwards, and C. W. Clark, **Phys. Rev. A** **96**, 023616 (2017).
- [92] Y.-H. Wang, T. Jacobson, M. Edwards, and C. W. Clark, **SciPost Phys.** **3**, 022 (2017).
- [93] The use of a well-defined initial state removes the vacuum ambiguity of a BHL [36].
- [94] A. Sinatra, C. Lobo, and Y. Castin, **J. Phys. B: At. Mol. Opt. Phys.** **35**, 3599 (2002).
- [95] M. Jacquet, M. Joly, F. Claude, L. Giacomelli, Q. Glorieux, A. Bramati, I. Carusotto, and E. Giacobino, **The**

- European Physical Journal D **76**, 152 (2022).
- [96] S. Butera and I. Carusotto, Phys. Rev. Lett. **130**, 241501 (2023).
- [97] K. Sacha, *Time crystals* (Springer International Publishing, Cham, Switzerland, 2020).
- [98] J. R. M. de Nova, D. Guéry-Odelin, F. Sols, and I. Zapata, New J. Phys. **16**, 123033 (2014).
- [99] J. R. M. de Nova, F. Sols, and I. Zapata, Annalen der Physik **529**, 1600385 (2017).
- [100] P. D. Drummond and M. Hillery, *The quantum theory of nonlinear optics* (Cambridge University Press, 2014).
- [101] H. S. Nguyen, D. Gerace, I. Carusotto, D. Sanvitto, E. Galopin, A. Lemaître, I. Sagnes, J. Bloch, and A. Amo, Phys. Rev. Lett. **114**, 036402 (2015).